The immunostimulatory activity of sea spray aerosols: bacteria and endotoxins activate TLR4, TLR2/6, NF-κB and IRF in human cells

Yunmeng Li, Wyona Schütte, Max Dekeukeleire, Colin Janssen, Nico Boon, Jana Asselman, Sarah Lebeer, Irina Spacova, Maarten De Rijcke

PII: S0048-9697(24)02112-0

DOI: https://doi.org/10.1016/j.scitotenv.2024.171969

Reference: STOTEN 171969

To appear in: *Science of the Total Environment*

Received date: 26 January 2024

Revised date: 11 March 2024

Accepted date: 23 March 2024

Please cite this article as: Y. Li, W. Schütte, M. Dekeukeleire, et al., The immunostimulatory activity of sea spray aerosols: bacteria and endotoxins activate TLR4, TLR2/6, NF-κB and IRF in human cells, *Science of the Total Environment* (2024), https://doi.org/10.1016/j.scitotenv.2024.171969

The immunostimulatory activity of sea spray aerosols: bacteria and endotoxins activate TLR4, TLR2/6, NF-κB and IRF in human cells

Yunmeng Li [a,b,c], Wyona Schütte [a], Max Dekeukeleire [b], Colin Janssen [c], Nico Boon [d], Jana Asselman [c], Sarah Lebeer [b], Irina Spacova [b], Maarten De Rijcke [a,*]

[a] *Flanders Marine Institute (VLIZ), InnovOcean Campus, Jacobsenstraat 1, 8400 Ostend, Belgium*

[b] *Laboratory of Applied Microbiology and Biotechnology, Department of Bioscience Engineering, University of Antwerp, Groenenborgerlaan 171, 2020 Antwerp, Belgium*

[c] *Blue Growth Research Lab, Ghent University, Wetenschapspark 1, 8400 Ostend, Belgium*

[d] *Center for Microbial Ecology and Technology (CMET), Ghent University, Coupure Links 653, 9000 Ghent, Belgium*

[*] Corresponding author at: Flanders Marine Institute (VLIZ), InnovOcean Campus, Jacobsenstraat 1, 8400 Ostend, Belgium.

E-mail address: maarten.de.rijcke@vliz.be (M. De Rijcke).

Abstract

Frequent exposure to sea spray aerosols (SSA) containing marine microorganisms and bioactive compounds may influence human health. However, little is known about potential immunostimulation by SSA exposure. This study focuses on the effects of marine bacteria and endotoxins in SSA on several receptors and transcription factors known to play a key role in the human innate immune system. SSA samples were collected in the field (Ostend, Belgium) or generated in the lab using a marine aerosol reference tank (MART). Samples were characterized by their sodium contents, total bacterial counts, and endotoxin concentrations. Human reporter cells were exposed to SSA to investigate the activation of toll-like receptor 4 (TLR4) in HEK-Blue hTLR4 cells and TLR2/6 in HEK-Blue hTLR2/6 cells, as well as the activation of nuclear factor kappa B (NF-κB) and interferon regulatory factors (IRF) in THP1-Dual monocytes. These responses were then correlated to the total bacterial counts and endotoxin concentrations to explore dose-effect relationships. Field SSA contained from 3.0 x 10^3 to 6.0 x 10^5 bacteria/m^3 air (averaging 2.0 ± 1.9 x10^5 bacteria/m^3 air) and an endotoxin concentration ranging from 7 to 1,217 EU/m^3 air (averaging 389 ± 434 EU/m^3 air). In contrast, MART SSA exhibited elevated levels of total bacterial count (from 2.0 x 10^5 to 2.4 x 10^6, averaging 7.3 ± 5.5 x10^5 cells/m^3 air) and endotoxin concentration from 536 to 2,191 (averaging 1,310 ± 513 EU/m^3 air). SSA samples differentially activated TLR4, TLR2/6, NF-κB and IRF. These immune responses correlated dose-dependently with the total bacterial counts, endotoxin levels, or both. This study sheds light on the immunostimulatory potential of SSA and its underlying mechanisms, highlighting the need for further research to deepen our understanding of the health implications of SSA exposure.

Keywords: Sea spray aerosols; Bacteria; Endotoxin; Immunostimulatory activity; Human cells

1. Introduction

Living near the ocean, particularly within 5 km, is increasingly linked to public health benefits. The primary evidence supporting this 'coastal health effect' comes from epidemiological studies that draw on self-reported metrics, such as general health and depression levels (Dempsey et al., 2018; Hooyberg et al., 2020; Wheeler et al., 2012). Clinical data regarding lower COVID-19 hospitalization rates at the Italian coast further underscore this link (Cascetta et al., 2021). While the exact mechanisms behind the mental and physical health benefits of living near the ocean remain unclear, the prevailing theories are that coastal environments alleviate perceived stress levels, promote social interactions, offer affordable exercise opportunities, and exhibit lower levels of air pollution (Hooyberg et al., 2023; White et al., 2016). Little attention has, however, been paid to the potential health benefits directly stemming from exposure to the vast array of marine microorganisms and bioactive compounds, despite many being recognized for their health-promoting properties in the food and pharmaceutical industries (Hamed et al., 2015; Suleria et al., 2016).

Humans can be exposed to marine microbes and their bioactive compounds through various routes, including ingestion (e.g., seafood), skin contact (e.g., sea bathing), and inhalation. The air in coastal environments is enriched with sea spray aerosols (SSA) that are generated by wave action and bubble bursting (De Leeuw et al., 2000). SSA carry various marine components into the atmosphere, including viruses, bacteria, fungi, phytoplankton, lipids, carbohydrates, amino acids, and vitamins (Aller et al., 2005; Mayol et al., 2014; Rastelli et al., 2017). With sizes ranging from 0.1 μm to 10 μm, SSA can remain suspended in the air for several days, traveling long distances via air mass movement before aging and eventually depositing (Gustafsson and Franzén, 2000; Su et al., 2022). Given the ubiquitous presence and size of SSA in coastal air, inhalation emerges as a frequent and continuous mode of exposure to marine substances and microorganisms for people living near the ocean. After inhalation, SSA can enter the human respiratory tract, extending from the upper airway all the way down to the alveolar region where they may enter the bloodstream and exert systemic effects (Cheng et al., 2005; Darquenne, 2012; Facciponte et al., 2018; Yu et al., 2022). Consequently, the regular inhalation of SSA might have a noticeable, yet overlooked, health effect on coastal residents.

The 'biogenics' hypothesis suggests that regular intermittent exposure to a mixture of airborne biogenic compounds in coastal environments exerts health benefits through the inhibition of the phosphoinositide 3-kinase (PI3K)/serine/threonine kinase Akt or protein kinase B PKB (Akt)/mammalian target of rapamycin complex 1 (mTORC1) systems (Moore, 2015). Overactivation of these cellular signaling pathways can trigger various pathological processes, leading to inflammation, diabetes, and cancer. Frequent down-regulation of these pathways is thought to reduce the risk of these diseases. A recent study exposed A549 human epithelial lung cells to SSA samples, revealing that SSA exposure indeed suppressed the overexpression of several mTOR-related genes (Asselman et al., 2019). This study provided the first *in vitro* evidence of potential health benefits caused by SSA and the molecular mechanisms involved. An organism-level study by Biddle et al. (2021) examined the effects of sea spray on the pulmonary health of mice, showing that exposure to Pacific Ocean spray elicited an increase in B cells in lung tissues. This recent finding suggests that SSA may also act as an immunological stimulant, warranting further investigation.

In humans, Toll-like receptors (TLRs) play a pivotal role in recognizing microbe-associated molecular patterns (MAMPs), initiating innate immune responses, and priming antigen-specific adaptive immunity (Kawai and Akira, 2010). TLR4, for example, interacts with lipopolysaccharides (LPSs) (also known as endotoxins) from the outer membranes of Gram-negative bacteria. TLR2, often forming heterodimers with either TLR1 or TLR6, recognizes a wide range of MAMPs including peptidoglycan and lipoteichoic acid (LTA) - both found in cell walls of Gram-positive bacteria – as well as lipoproteins and lipopeptides present in the cell membranes of both Gram-positive and Gram-negative bacteria (Kang et al., 2016). Activation of TLRs triggers cellular signaling cascades involving downstream transcription factors like nuclear factor kappa B (NF-κB) and interferon regulatory factors (IRF), which in turn regulate inflammation-related gene expression and promote the release of immunostimulatory cytokines and interferons.

Several LPSs and lipid A components (the toxic moiety of LPS) isolated from marine bacterial strains exhibit weak agonistic activities on TLR4-dependent NF-κB activation, and show inhibitory effects against pathogenic LPS-induced NF-κB activation (Di Lorenzo et al., 2018, 2017; Pither et al., 2021).

This, along with the detection of endotoxins in SSA over coastal areas (Lang-Yona et al., 2014) and the abundance of Gram-negative bacteria in SSA (Cho and Hwang, 2011), motivated us to investigate the effects of Gram-negative bacterial endotoxin in SSA on TLR4. We extend our study to include TLR2/6, which covers the effects of Gram-positive bacterial components, as well as NF-κB and IRF, which are activated by other upstream immune receptors (e.g., TLR3 recognizing viral dsRNA, TLR5 recognizing bacterial flagellin) (Kawai and Akira, 2010). In this study, we aim to 1) analyze how marine bacteria and endotoxins in SSA interact with TLR4 and TLR2/6, and 2) gain insights into broader immunological aspects at the level of transcription factors considering the complexity of SSA components and their effects beyond receptors activation. To accomplish this, we collected SSA in the field and under laboratory-controlled conditions, and characterized their contents (sodium, total bacterial counts, and endotoxin concentrations). Samples were then used to determine their effects on human reporter cell lines by measuring the activation of TLR4, TLR2/6, NF-κB, and IRF. These cellular immune responses were subsequently correlated with total bacterial counts and endotoxin concentrations to explore potential dose-response relationships.

2. Materials and methods

2.1. SSA collection

SSA were collected over a four-week period, from March 20 to April 13, 2023 in Ostend, Belgium. Sampling occurred on eight distinct days, evenly split across four weeks, with one day each week dedicated to collecting field SSA and one to generate SSA in the laboratory using a marine aerosol reference tank (MART). The MART, constructed as a breaking wave analogue based on methodologies detailed in previous studies (Stokes et al., 2013; Van Acker et al., 2021b), facilitates repeatable SSA generation that mimics oceanic conditions in a controlled environment. Further information on the MART system set-up and settings can be found in **Fig. S1**. The MART was filled with natural seawater collected from Ostend beach next to the field SSA sampling site. The local water residence time is around 7 days (Belgische Staat, 2018). Thus, our approach ensures that

MART-generated SSA (hereafter referred to as 'MART samples') originate from the same water mass as the field SSA samples (subsequently termed 'Field samples') collected within the same week. We anticipated that MART samples, relative to Field samples from the same week, would exhibit a higher biomass and less influence from terrestrial air and/or anthropogenic activities.

Field SSA sampling was conducted on the harbor wall of Ostend (HO; 51°14'28"N, 2°55'27"E; directly adjacent to the sea), when the wind speed exceeded 4 m/s and SSA production is expected (**Fig. 1 (a)**). Environmental parameters, including ocean variables such as wave height, measured by the 'Ostend eastern palisade - Buoy' (51°14'48"N, 2°55'39"E; approximately 600 m distance from HO) and meteorological conditions recorded by 'Ostend - Weather station' (51°14'15"N, 2°55'48"E; about 400 m from HO) (**Fig. 1 (a)**), were sourced from the public database '*Meetnet Vlaamse Banken*' (https://meetnetvlaamsebanken.be/) and are summarized in **Table S2**. A Coriolis µ microbial air sampler (Bertin Technologies; henceforth 'Coriolis sampler'), positioned 1 m above ground level on a tripod with its inlet facing the wind, was used for sampling (**Fig. 1 (b)**). Operating on the cyclonic liquid impingement principle, it draws air into a cone containing 15 mL of collection liquid, creating a vortex that propels particles against the wet cone wall, thereby concentrating them in the liquid. We sampled for one hour per sample (besides sample F3b, which accidentally ran for 2 hours; **Table S1**). We used Milli-Q water (Merck-Millipore) as the collection liquid and operated the Coriolis sampler at its maximum air flow rate of 300 L/min. The 15 mL of Milli-Q water in the cones was initially prepared within a laminar flow hood (Thermo Scientific) in the laboratory. To mitigate any effect from re-aerosolization and evaporation loss during sampling, a known issue for this sampler, the collection liquid in the cones was manually topped up three times to 15 mL (every 20 minutes). This was done using a 50 mL syringe (Merck-Millipore) filled with the same Milli-Q water attached to the 25 mm inlet that is foreseen for this purpose. Post-sampling, samples were kept in a cold box for transport to the laboratory, where they were transferred to 15 mL Falcon conical centrifuge tubes (Fisher Scientific) for storage at 4 °C until analysis. Five replicates were collected each day, except for Week 1, where it started raining after four hours and sampling was terminated earlier. All devices and consumables were pretreated by washing with 1% (v/v) HNO_3 (Merck-Millipore; percent purity

65%), 70% (v/v) EtOH (Chem-Lab), and Milli-Q water to remove potential contamination with salt and bacteria, followed by overnight drying in a laminar flow hood. The Milli-Q water, treated identical to the SSA samples but not used in actual SSA collection, served as a blank. In total, 19 Field samples and 4 Field blanks were collected.

MART SSA sampling was carried out in a climate-controlled room (maintained at 18 ℃) at the Marine Station Ostend (MSO; 51°14'10"N, 2°55'42"E) (**Fig. 1 (a, c)**). Prior to each use, the MART was cleaned, involving three rounds of cleansing with Decon 90 (Decon Laboratories Limited) and Milli-Q water, followed by a 70% EtOH spray, and a final rinse with Milli-Q water before air drying. A total of 150 L of seawater was collected from Ostend beach (51°14'28"N, 2°55'56"E, about 400 m from HO) (**Fig. 1 (a)**) and filtered using a 100 μm sieve (VWR; sieve frame diameter, 203.2 mm) to remove larger debris. The filtered seawater was then transferred to six 25 L bottles (Nalgene) for transport to the laboratory. Upon allowing 30 minutes of sedimentation for sand and other particles, the seawater situated more than 5 cm above the bottom of the bottle was transferred to the MART via siphoning, amounting to a total of 120 L. The MART was then run for one hour to saturate any room air inside with produced SSA. Next, the Coriolis sampler was connected to the MART for focused SSA sampling, which mirrored the field sampling methods. Each sampling day yielded 5 replicates. A total of 20 MART samples and 4 MART blanks were collected.

In summary, four sets of both MART and field SSA sampling activities were executed using a Coriolis sampler, resulting in 19 Field samples, 4 Field blanks, 20 MART samples, and 4 MART blanks. Samples were stored at 4 ℃ to suppress bacterial growth, prevent endotoxin degradation, and maintain their overall activity. The decision to store samples at 4 ℃ is based on this temperature's effectiveness in reducing the metabolic activity of bacteria and slowing down any degradation processes that could compromise the integrity of endotoxins and other sensitive components. We deliberately chose to avoid freezing to prevent ice crystal formation, which could damage cellular structures and disrupt the bioactivity of certain molecules (Hubel et al., 2014). The PyroGene Recombinant Factor C (rFC) assay (Lonza), used for endotoxin measurements in our study, recommends storing its reagents (including *E. coli* LPS standards) within the 2-8 ℃ range. This

recommendation further supports our storage protocol, ensuring the stability and bioactivity of endotoxins in the samples.

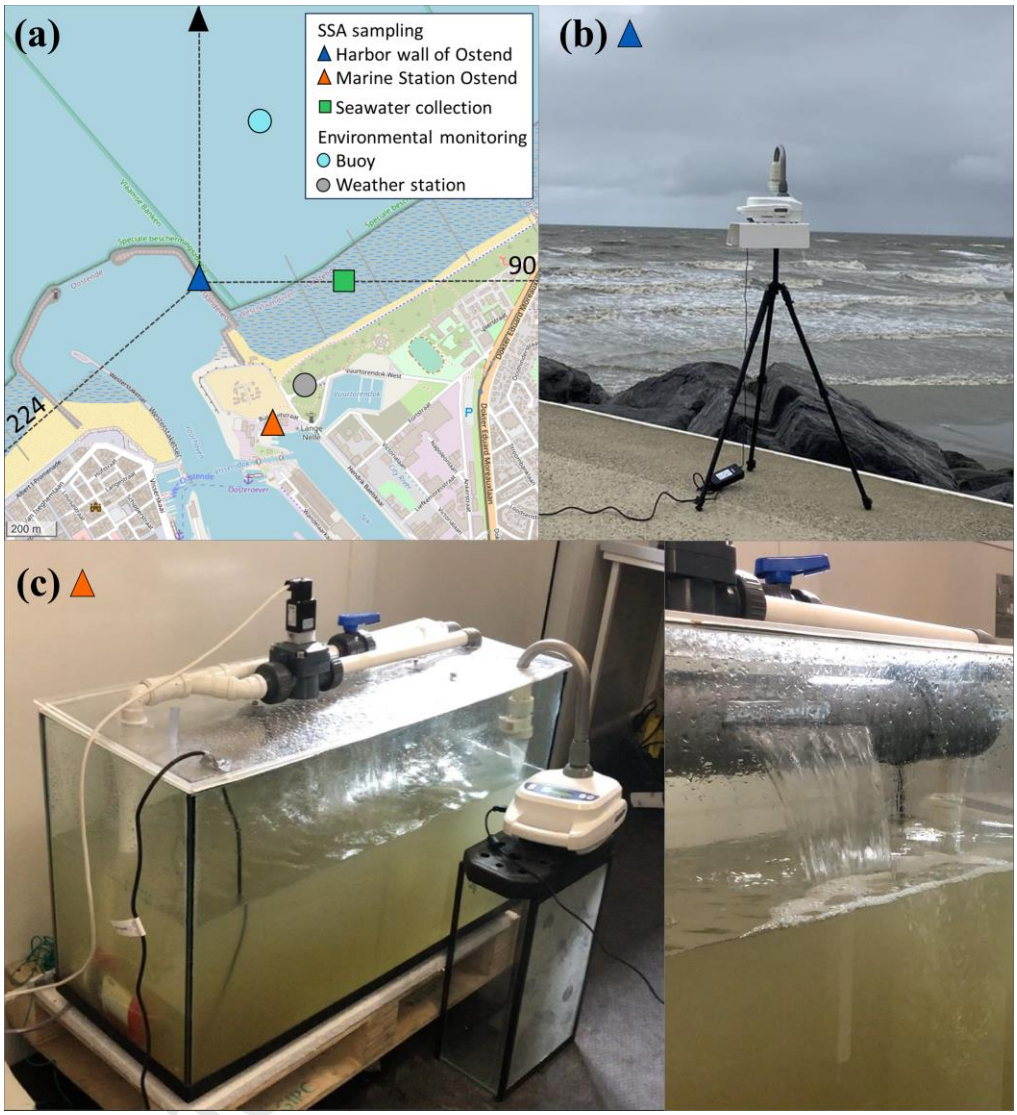

Fig. 1. (a) Map showing the locations of field sea spray aerosols (SSA) sampling on the harbor wall of Ostend (HO), the Marine Station Ostend (MSO), the seawater collection site for laboratory SSA generation, and the local environmental monitoring stations (Buoy and Weather station). Sea wind directions for HO are between ≥224° and ≤90°. (b) Field SSA sampling on the HO using a Coriolis sampler. (c) SSA generation at the MSO using a marine aerosol reference tank (MART).

2.2. SSA characterization

To validate that our Field samples predominantly contained SSA, we 1) reviewed the wind direction data recorded by a local weather station, 2) conducted a 72-hour backward trajectory analysis of air mass transport at the sampling height using the Hybrid Single-Particle Lagrangian Integrated Trajectory (HYSPLIT) model developed by the United States National Oceanic and Atmospheric Administration (NOAA) with meteorological data from the Global Data Assimilation System (GDAS) data (Stein et al., 2015), 3) analyzed the correlations between the sodium (Na) content, total bacterial count, and endotoxin concentration using simple linear regression analysis, and 4) compared them to the correlations observed in MART samples.

Sodium (Na), a proxy for the amount of SSA collected, was measured by acidifying 5 mL subsamples using 65% (v/v) HNO_3 to achieve a final concentration of 1% HNO_3. This was followed by filtration through 0.45 µm PES syringe filters (Novolab). After filtration, the sodium ion concentration (µg/mL) was determined using inductively coupled plasma optical emission spectroscopy (Thermo Scientific iCAP 7000 series), as described in (Van Acker et al., 2021a).

Bacterial counts were measured using an Accuri C6 flow cytometry (BD Biosciences) with an autoloader, based on the methods described in (Van Nevel et al., 2013) and (Nescerecka et al., 2016). Subsamples of 200 µL were loaded into a 96-well plate (VWR), stained with 2 µL of SYBR Green I (SG, 10,000 times diluted from stock with Tris buffer; Invitrogen) combined with propidium iodide (PI, 6 µM final concentration; Invitrogen), and then incubated in the dark at 37°C for 20 minutes. Subsequently, 25 µL of each sample was analyzed using the Fast mode with a flow rate of 66 µL/min. Milli-Q water and one heat-killed sample (incubated at 80°C for 10 minutes) were used as negative and positive controls, respectively. Damaged and intact cells were counted separately by gating on green (FITC-A) vs. red (PerCP-A) fluorescence plots in the BD CSampler Plus software (BD Biosciences). The total bacterial count (cells/mL) was calculated by combining these two values.

Endotoxin concentrations (endotoxin units (EU)/mL) were determined using the PyroGene Recombinant Factor C (rFC) assay (Lonza). This assay employs the rFC protein, a protease

proenzyme that activates upon binding to endotoxins, triggering the hydrolysis of a synthetic substrate and resulting in the emission of a fluorescent signal. These signals were detected using a fluorescence microplate reader (SpectraMax iD3, Avantor, VWR) at excitation and emission wavelengths of 380 and 440 nm, respectively. For this assay, 2 mL subsamples were filtrated through 0.45 μm PES syringe filters and then diluted with non-pyrogenic water (Lonza). The detection process was conducted as per the manufacturer's instructions, as previously described in (Moretti et al., 2018). Briefly, 100 μL of each sample, along with 8 standard points (ranging from 0.005 to 10 EU/mL, prepared using 20 EU/mL *Escherichia coli* LPS (O55:B5) in non-pyrogenic water), and a non-pyrogenic water blank were loaded in duplicates into a sterilized, black-walled 96-well plate (VWR). After a 10-minute incubation at 37 ℃, 100 μL of a freshly prepared working solution containing fluorogenic substrate, assay buffer, and rFC enzyme in a 5:4:1 ratio was added to each well. Initial fluorescence readings (t = 0 min) were taken, followed by a second reading after a 60-minute incubation at 37 ℃ (t = 60 min). Background fluorescence (t = 0 min) was subtracted, and the log values of fluorescence for the standards was plotted against their log endotoxin concentrations, achieving an $R^2 > 0.998$. The derived standard curve equation was used to determine the endotoxin concentrations of diluted samples. The original concentrations in the samples were then calculated by multiplying these values by their respective dilution factors.

All SSA samples and blanks were measured for their Na contents, total bacterial counts, and endotoxin concentrations. The measurements in the liquid samples (*/mL) were converted to air concentrations (*/m^3 air) by first subtracting the blank values, then multiplying by the total liquid volume (15 mL), and finally dividing by the sampled air volume (18 m^3).

2.3. Cell culture

Three human reporter cell lines (Invivogen) were used. HEK-Blue hTLR4 and HEK-Blue hTLR2/6 cells were cultured in Dulbecco's Modified Eagle Medium (DMEM) (Gibco) with 4.5 g/L glucose (Gibco), 2 mM L-glutamine (Gibco), 10% (v/v) heat-inactivated fetal bovine serum (FBS Premium+, endotoxin-free) (Gibco), normocin (100 μg/mL) (Invivogen), PenStrep (100 μg/mL) (Gibco) and HEK-Blue Selection (Invivogen). THP1-Dual cells were cultured in Roswell Park Memorial Institute

(RPMI) 1640 medium (R1145-500ML; Sigma Aldrich) with L-glutamine supplemented with 25 mM HEPES buffer (Gibco), 10% (v/v) heat-inactivated fetal bovine serum (FBS Premium+, endotoxin-free), normocin (100 µg/mL), PenStrep (100 µg/mL) and Blasticidin and Zeocin as selection markers (Invivogen). All cells were cultivated at 37 °C in a humidified incubator containing 5% (v/v) CO_2 (Memmert).

2.4. Activation of TLR4, TLR2/6, NF-κB, and IRF in human reporter cell lines

HEK-Blue hTLR4 cells and HEK-Blue hTLR2/6 cells, both derived from human embryonic kidney (HEK 293) cells, were specifically engineered to study the responses of TLR4 and TLR2/6, respectively. Upon stimulation with specific ligands, the relevant TLRs are activated, subsequently triggering both NF-κB and activator protein 1 (AP-1). This cascade leads to the production of secreted embryonic alkaline phosphatase (SEAP). The SEAP levels, which signify the activation intensity of the TLR4 and TLR2/6, can be assessed by measuring the optical density (OD) at 405 nm following the addition of p-nitrophenyl phosphate (pNPP; Thermo Scientific) solution. Similarly, THP1-Dual cells, originated from human THP-1 monocytes, allow for simultaneous assessment of NF-κB (via SEAP) and IRF (via luciferase) activation. The SEAP levels, reflecting NF-κB activity, can be measured using the aforementioned method. Luciferase activity, indicating IRF activation, is quantifiable in luminescence units at 600 nm after introducing the QUANTI-Luc buffer (Thermo Scientific).

One day before the exposure experiment, HEK-Blue hTLR4 and HEK-Blue hTLR2/6 cells were seeded into 96-well plates (VWR) at 100 µL per well at approximately 1.5 x 10^6 live cells/mL in regular DMEM culturing medium and incubated for 24 hours until approximately 90% confluent. After incubation, the medium was removed from the adherent cells using a vacuum hand operator (Integra) and replaced with 100 µL of 2x concentrated DMEM (without FBS, normocin, or selective marker). The 2x concentrated DMEM was formulated from a 10x DMEM medium (D2429-100ML; Sigma Aldrich) with added ultrapure water (Invitrogen), 1.168 g/L L-glutamine, 0.008 g/L folic acid and 0.75% (v/v) sodium bicarbonate (Gibco). Similarly, on the exposure day, the regular RPMI culturing medium from non-adherent THP1-Dual cells was removed post-centrifugation at 300 x *g*.

The cells were then resuspended in 2x concentrated RPMI, formulated from a 10x RPMI medium, ultrapure water, 1.168 g/L L-glutamine and 0.75% sodium bicarbonate. These THP1-Dual cells were then seeded into 96-well plates at 100 µL per well at 10^6 live cells/mL. For all cell lines, the 2x concentrated medium compensated for the dilution effect incurred when adding SSA samples (presented in the collection liquid). To ensure assay validity, we added agonists as positive controls. Specifically, *E. coli* O111:B4 LPS (Sigma Aldrich) was used as the agonist for both HEK-Blue hTLR4 and THP1-Dual cells, while Pam2CSK4 (a synthetic diacylated lipopeptide; Invivogen) was used for HEK-Blue hTLR2/6 cells. Ultrapure water served as negative control. 100 µL per well of each treatment (negative control, positive control or sample) were added at room temperature and in duplicates to the designated wells containing cell cultures. Following an approximately 24-hour incubation at 37°C in a humidified 5% CO_2 incubator, activations of TLR4, TLR2/6, NF-κB, and IRF were quantified. This was achieved by transferring 50 µL of cell supernatant from each well to fresh 96-well plates and adding either 100 µL of pNPP solution or QUANTI-Luc buffer. After an incubation of 5-40 minutes (based on the observed color reaction) in the dark at room temperature, the signals were read out using a Synergy HTX Multi-Mode reader (BioTek). The average fluorescence or luminescence of the duplicates was then calculated for each sample. The specific immunostimulatory effects of SSA were calculated by subtracting the responses to Milli-Q controls from the inductions caused by the samples of that week.

2.5. Statistical analysis

Differences in sodium content, total bacterial count, and endotoxin concentration among groups (sampling site and sampling week) were evaluated using the Kruskal-Wallis test, followed by the Wilcoxon rank sum test for post-hoc comparison. Simple linear regression analysis was conducted to explore the relationships between sodium content, total bacterial count, and endotoxin concentration. Multiple linear regression analysis was used to evaluate the influence of total bacterial count and endotoxin concentration on cellular immune responses. The data were $\log_{10}$-transformed to reduce skewness and increase linearity. The robustness of the regression models was assessed by using the variance inflation factor for collinearity testing, and the Shapiro-Wilk, Breusch-Pagan, and Box-

Pierce tests to determine normality, homoscedasticity, and independence of residuals, respectively. All data analyses were performed using R (version 4.2.2) with packages car (Fox and Weisberg, 2011) and lmtest (Zeileis and Hothorn, 2002). The significance level of 0.05 was used for all tests.

3. Results

3.1. Identification and characterization of SSA samples

A total of 18 Field and 18 MART SSA samples collected and characterized regarding their sodium (Na) contents, total bacterial counts, and endotoxin concentrations (**Table S1**). MART samples generally contained more Na than Field samples (**Fig. 2 (a)**, $p < 0.05$ for Weeks 1, 3, and 4; $p = 0.057$ for Week 2). MART samples of Weeks 1, 2, and 4 also exhibited elevated total bacterial counts and endotoxin concentrations compared to Field samples (Week 1, both $p < 0.05$; Week 2, $p = 0.40$ and $p = 0.057$ respectively; Week 4, both $p < 0.01$), while Week 3 showed comparable levels ($p = 0.70$ and $p = 1.00$, respectively) (**Fig. 2 (b, c)**). The latter observation led us to suspect that Week 3 Field samples could be affected by terrestrial air and/or anthropogenic activities. This supposition was supported by local meteorological data (**Table S2**) and air mass back trajectories analyzed using the HYSPLIT model and GDAS data (**Fig. 3**). A local weather station observed that wind directions for Week 1 (229 ± 6° (minimum 220, maximum 237)), Week 2 (239 ± 5° (234, 247)), and Week 4 (260 ± 8° (253, 272)) were within the sea wind range (between ≥224° and ≤90°) for the field sampling site (**Table S2, Fig. 1 (a)**), while predicted trajectories using the HYSPLIT model demonstrated that the air masses sampled during Weeks 1, 2, and 4 had recently passed across marine systems (**Fig. 3 (a, b, d)**). In contrast, the wind direction for Week 3 (70 ± 14° (51, 253)) showed an orientation encompassing both land and sea (**Table S2, Fig. 1 (a)**), and the air mass predominantly came from across terrestrial environments (**Fig. 3 (c)**).

Fig. 2 (d, e, f) shows simple linear regressions between the Na content, total bacterial count, and endotoxin concentration in our samples. For Weeks 1, 2, and 4, significant correlations between Na content and total bacterial count ($p < 0.001$ and $R^2 = 0.64$), Na content and endotoxin concentration (p

< 0.001 and $R^2 = 0.66$), and the total bacterial count and endotoxin concentration ($p < 0.001$ and $R^2 = 0.54$) were found across both Field and MART samples. The Week 3 Field samples deviated from each of these trends, further suggesting a non-marine origin of the bacteria and endotoxins. Week 3 Field samples (5 samples) were excluded from subsequent immunostimulatory tests because of this.

Week 3 MART samples aligned with the correlation line between Na content and total bacterial count, while this was not the case for the correlation lines for Na content and endotoxin concentration, and the total bacterial count and endotoxin concentration (**Fig. 2 (d, e, f)**). This deviation could be due to the extremely high endotoxin concentrations in Week 3 MART samples (5,888 ± 1440 EU/m^3 air), which were 3-6 times higher than in other weeks (Week 1, 1,784 ± 316 EU/m^3 air; Week 2, 1,084 ± 306 EU/m^3 air; Week 4, 972 ± 400 EU/m^3 air) (**Fig. 2 (c, f), Table S1**). We suspect that the high levels of endotoxin in Week 3 MART samples may be caused by increased riverine runoff due to precipitation or the disturbance of harbor sediments by vessel traffic. After reviewing our personal observations of the seawater conditions (e.g., turbidity, the visible occurrence of algae, level of foam on the beach) and local weather data such as wave height and precipitation, we found no evidence to adequately explain the observed spike in endotoxin levels in the Week 3 MART samples. Considering the unusual and unexplained spike in endotoxin levels in Week 3 MART samples, these samples (5 samples) were also excluded from subsequent immunostimulatory tests to avoid potential confounding effects on the results.

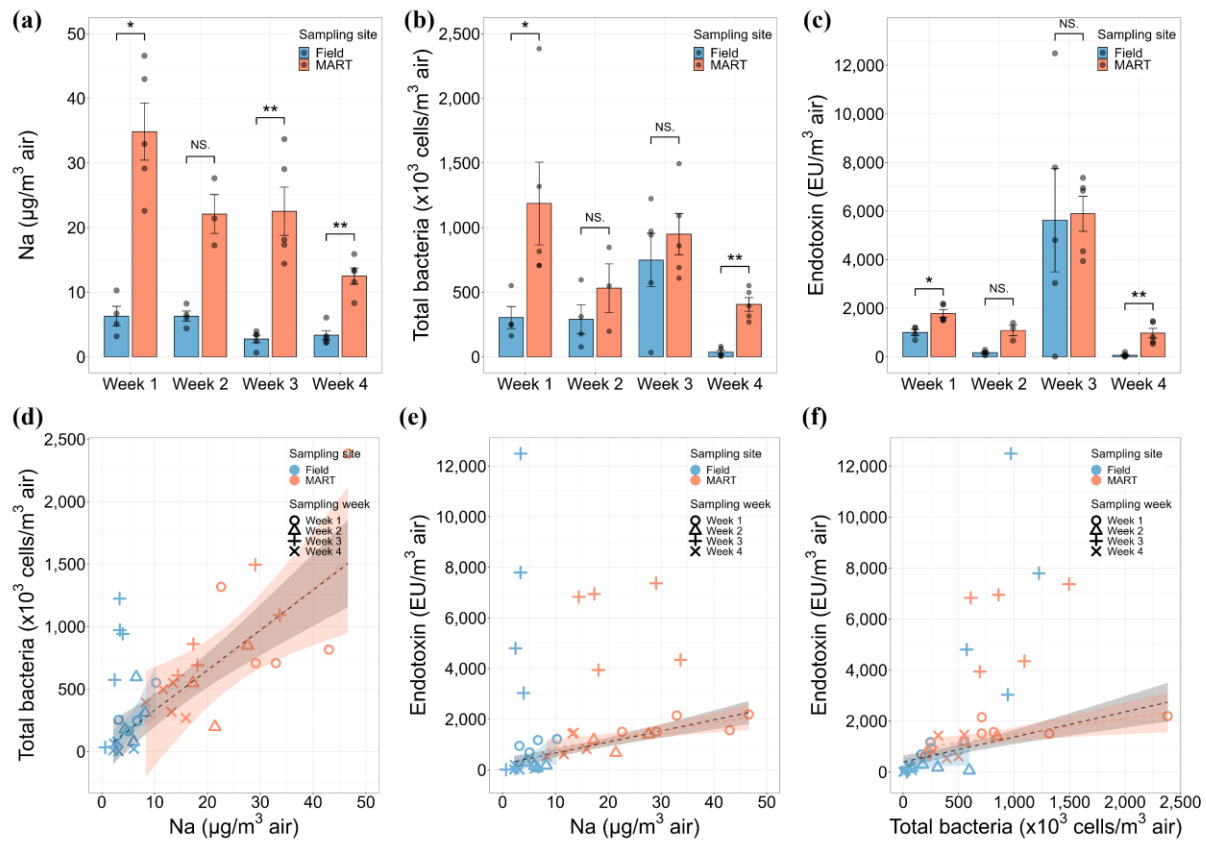

Fig. 2. Bar plots displaying (a) sodium (Na) content, (b) total bacterial count, and (c) endotoxin concentration in sea spray aerosols (SSA) samples collected from different sites (Field and MART) across different weeks (Weeks 1, 2, 3, and 4). Differences among groups were tested using the Kruskal-Wallis test followed by the Wilcoxon rank sum test. NS., not significant; *, $p < 0.05$; **, $p < 0.01$. Linear regression correlations with 95% confidence intervals between (d) Na content and total bacterial count, (e) Na content and endotoxin concentration, and (f) total bacterial count and endotoxin concentration were added as dashed lines. Regression lines for Field samples, MART samples, and combined samples were colored blue, orange, and black, respectively. Week 3 data were omitted from these regression analyses due to suspected terrestrial origins.

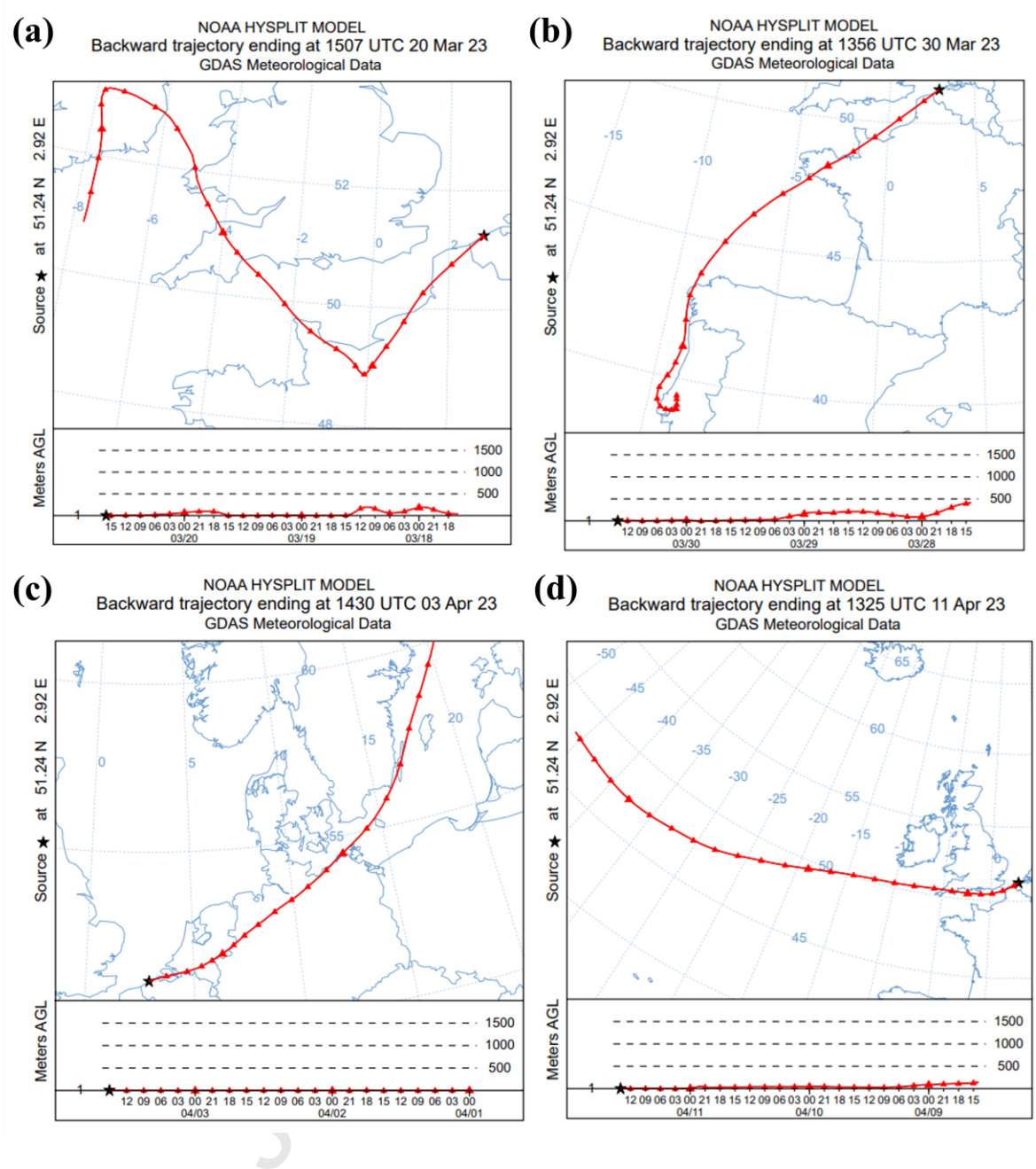

Fig. 3. 72-hour back trajectories of air masses arriving at the sampling height on the harbor wall of Ostend (HO) for each field sampling period in (a) Week 1, (b) Week 2, (c) Week 3, and (d) Week 4. These trajectories were calculated using the Hybrid Single-Particle Lagrangian Integrated Trajectory model (HYSPLIT) model with Global Data Assimilation System (GDAS) meteorological data.

3.2. SSA activated TLR4, TLR2/6, NF-κB, and IRF in human reporter cells dose-dependently linked to total bacterial count and endotoxin concentration

All SSA samples (including 13 MART samples and 13 Field samples) from Weeks 1, 2, and 4, along with Milli-Q water (used as the collection liquid), were assessed for their immunostimulatory potential. The evaluation process involved specific human cell lines: HEK-Blue hTLR4 cells for assessing TLR4 receptor induction, HEK-Blue hTLR2/6 cells for TLR2/6 receptor induction, and THP1-Dual cells for both NF-κB and IRF transcription factors inductions. The validity of the experiment was ensured by using known agonists for these cell lines (*E. coli* O111:B4 LPS for HEK-Blue hTLR4 cells and THP1-Dual cells, and Pam2CSK4 for HEK-Blue hTLR2/6 cells).

The induction levels of TLR4, TLR2/6, NF-κB, and IRF in collection liquid Milli-Q water controls matched those of the ultrapure water serving as negative controls in the immunostimulatory tests, indicating no contamination in the collection liquid. Except NF-κB induction by F4e and IRF induction by F4a, all inductions from SSA samples were above zero, indicating the activation of TLR4, TLR2/6, NF-κB, and IRF by both Field and MART samples. **Fig. 4** displays simple linear regressions between $\log_{10}$-transformed activations of these receptors and transcription factors in the respective cells and $\log_{10}$-transformed total bacterial count and endotoxin concentration. The activation of TLR4, TLR2/6, NF-κB, and IRF showed significantly positive correlations with both total bacterial count and endotoxin concentration (all $p < 0.001$ and $R^2 \geq 0.55$), demonstrating dose-dependent effects. To explore which factor, total bacterial count or endotoxin concentration, was the main driver for the activation of the observed responses, we performed a multiple linear regression analysis (**Table 1**). Checks for the model assumptions revealed issues with homoscedasticity in the TLR4 and TLR2/6 models, normality concerns in the NF-κB model, and both homoscedasticity and independence of residuals in the IRF model. However, removing one or two outliers (as identified by the Cook's Distance) rectifies all violations of the models' assumptions. Results of the multiple linear regression showed TLR4 activation to be significantly affected by both total bacterial count and endotoxin concentration (both $p < 0.05$). In contrast, TLR2/6, NF-κB and IRF activations were only significantly predicted by total bacterial count.

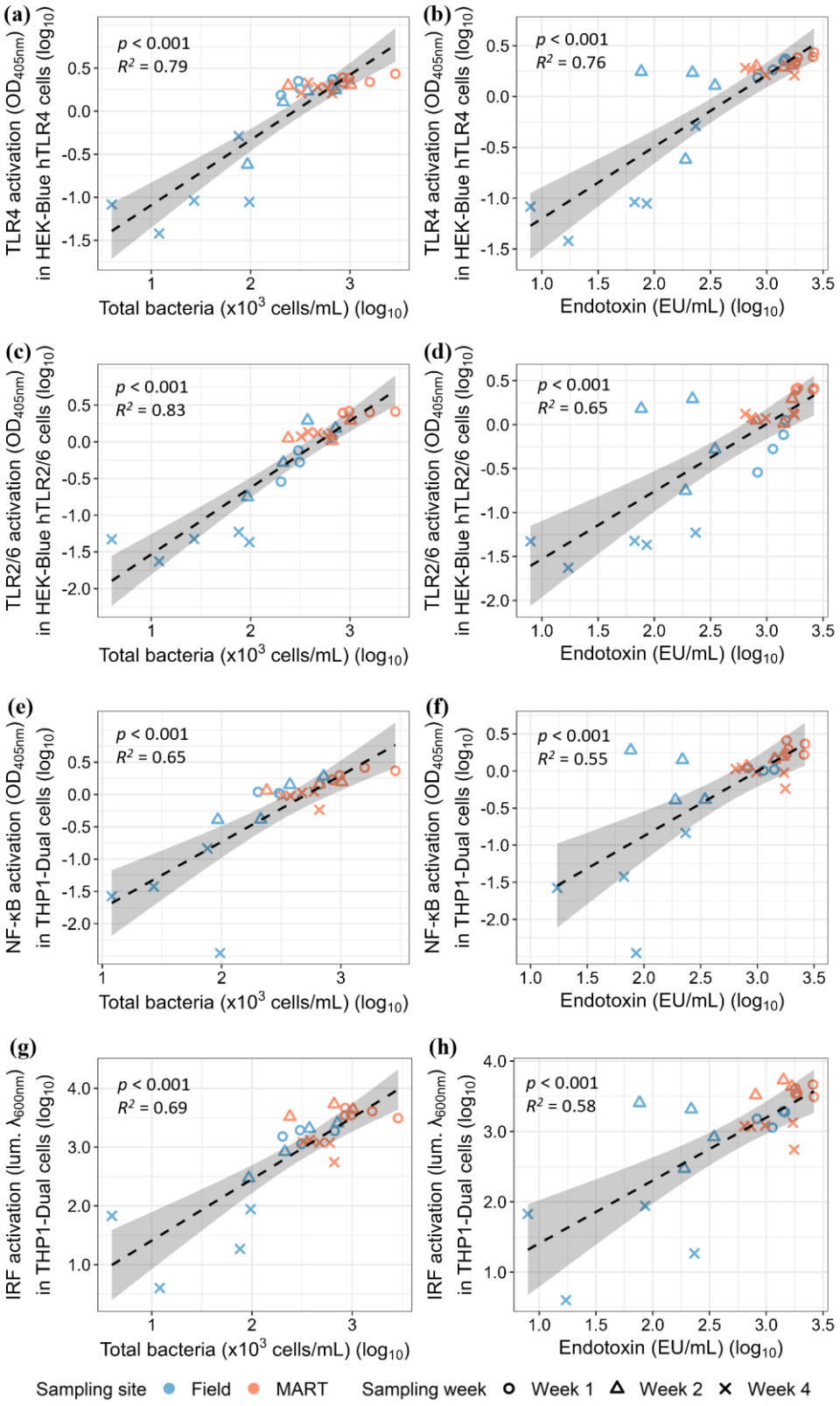

Fig. 4. Linear regressions with 95% confidence intervals between $\log_{10}$-transformed values of total bacterial count and endotoxin concentration with the activations of TLR4 in HEK-Blue hTLR4 cells, TLR2/6 in HEK-Blue hTLR2/6 cells, and NF-κB and IRF in THP1-Dual cells, induced by SSA.

Table 1

Multiple linear regression analysis of total bacterial count and endotoxin concentration in sea spray aerosols (SSA) affecting the activation of TLR4 in HEK-Blue hTLR4 cells, TLR2/6 in HEK-Blue hTLR2/6 cells, as well as NF-κB and IRF in THP1-Dual cells.

Dependent variable	Independent variables	Diagnostic checks	R^2	*p*	Coefficients	
					Estimate	*p*
TLR4 activation	Intercept	abd	0.83	<0.001	-2.00	<0.001
	[Bacteria]	c, $p = 0.005$			0.46	**0.006**
	[Endotoxin]				0.33	**0.032**
TLR2/6 activation	Intercept	abd	0.83	<0.001	-2.47	<0.001
	[Bacteria]	c, $p = 0.031$			0.85	**<0.001**
	[Endotoxin]				0.06	0.713
NF-κB activation	Intercept	acd	0.67	<0.001	-2.96	<0.001
	[Bacteria]	b, $p < 0.001$			0.76	**0.010**
	[Endotoxin]				0.30	0.236
IRF activation	Intercept	ab	0.70	<0.001	0.27	0.498
	[Bacteria]	c, $p = 0.006$			0.86	**0.007**
	[Endotoxin]	d, $p = 0.028$			0.20	0.466

Diagnostic Checks: a. Collinearity of independent variables assessed by variance inflation factor (VIF), with VIF < 5 indicating no significant collinearity; b. Normal distribution of the model's residuals assessed by the Shapiro-Wilk test, with $p > 0.05$ indicating normality; c. Homoscedasticity assessed by the Breusch-Pagan test, with $p > 0.05$ indicating homoscedastic residuals of the model; d. Independence of the model's residuals assessed by the Box-Pierce test, with $p > 0.05$ indicating independent residuals.

4. Discussion

This study is the first to investigate the immunostimulatory potential of SSA with a focus on the roles of marine bacteria and their endotoxins. We observed that SSA samples activated the important MAMP-sensing receptors TLR4 and TLR2/6 in human reporter cells, and induced transcription factors NF-κB and IRF which initiate downstream immune responses. The activity of all these immune markers increased with total bacterial counts (ranging from 3 x 10^3 to 2.4 x10^6 cells/m^3 air) and endotoxin concentrations (ranging from 7 to 2,191 EU/m^3 air) in a dose-dependent manner. These findings reveal the role of SSA in immune activation, providing additional mechanistic support for the 'coastal health effect'. Considering NF-κB and IRF act as metabolic switches in the mTOR pathway, our results also add support to the 'biogenics' hypothesis of Moore (2015).

Existing studies on the interactions between MAMPs and TLRs have largely focused on pure bacterial strains and their isolated MAMPs. Although high endotoxin levels in environmental aerosols (particularly those from urban and industrial aerosols) have been associated with elevated TLR4 activation, a direct correlation between endotoxin levels and TLR4-mediated immune recognition is rarely established in the literature (Hetland et al., 2005; Steerenberg et al., 2004). A recent study by Moretti et al. (2019) advanced this field by demonstrating a dose-dependent TLR4 activation in HEK-Blue hTLR4 cells in response to varying endotoxin concentrations in urban aerosols. Building on this work, our study expands the scope of investigation to SSA. With their distinct origin and composition, SSA provide a unique opportunity to further explore and understand the dynamics of MAMPs-TLRs interactions within a marine context. We used a multiple linear regression analysis to examine the relationship between total bacterial count and endotoxin concentration in SSA with the activation of TLR4 and TLR2/6, aiming to determine whether these TLRs recognize MAMPs within SSA. In addition, we explored the activation of NF-κB and IRF, providing a deeper insight into the immune responses stimulated by SSA at the transcription factor level.

Both endotoxin concentrations and total bacterial counts in SSA significantly affected TLR4 activation (**Table 1**). This aligns with the known immunostimulatory properties of endotoxins (Liebers et al., 2008) and the fact that there is a large proportion of Gram-negative species among

marine bacteria (Cho and Hwang, 2011). A similar influence of total bacterial count on TLR2/6 activation was observed (**Table 1**), consistent with the known specificity of TLR2/6 responding to a broader array of components from both Gram-negative and Gram-positive bacteria. No significant influence of endotoxin concentration on TLR2/6 activation was observed (**Table 1**), aligning with the inherent characteristics of TLR2/6 not recognizing common endotoxins. The activation of both transcription factors NF-κB and IRF were influenced by total bacterial count (**Table 1**), while no significant responses to endotoxin concentration were detected. This suggests that the activation of these transcription factors is more susceptible to the combined effects of various bacterial components present at higher bacterial counts, rather than endotoxin concentration alone. Indeed, NF-κB and IRF can be activated by a wide array of microbial stimuli beyond endotoxins (Claes et al., 2012; Kusiak and Brady, 2022; Spacova et al., 2023; Taniguchi et al., 2001). These findings extend the current understanding of MAMPs-TLRs interactions from marine bacteria beyond the context of pure strains and isolated MAMPs towards complex bacteria-mediated effects of SSA exposure, demonstrating dose-dependent immune activation by SSA. The taxon-specific structure of LPS as well as other SSA components like LTA can affect TLR4, TLR2/6, NF-κB and IRF activation (Claes et al., 2012; Erridge et al., 2002), and will change the immunostimulatory properties of SSA. The absence of bacterial types (e.g., Gram-positive, Gram-negative) and LTA measurements in this study limits our understanding of the correlation between marine Gram-positive bacteria and the activation of TLR2/6, NF-κB and IRF. In addition to the SSA endotoxin concentrations quantified in our study, we therefore recommend future studies on the immunological health effects of SSA to include characterization of bacterial communities and their count in SSA and measurements of LTA and other MAMPs like flagellin and dsRNA. Further dissecting the roles of dissolved versus cell-attached components like endotoxin, possibly through the utilization of filtration-sterilized SSA samples, will provide clearer insights into their distinct immunostimulatory contributions. Effective analysis of the above-mentioned SSA components necessitates high-biomass samples, a challenging yet crucial task in this research field. Methodological advancements, such as using multiple air samplers to collect SSA simultaneously and pooling samples to increase the available biomass, would be a solution.

Considering the limited complexity and scope of our study, it is challenging to place our observations on immunostimulation by SSA within the broader contexts of general immune response research and the 'coastal health benefits'. Studies increasingly report that pure marine bacterial strains and their isolated derivatives (LPS, lipid A) cause weaker stimulation of TLR4-dependent NF-κB and downstream cytokines such as TNF-α, IL-6, and IL-8 compared to pathogenic *E. coli* LPS, and may even inhibit responses to pathogenic LPS (Carillo et al., 2011; Di Lorenzo et al., 2018, 2017; Kokoulin et al., 2016; Maaetoft-Udsen et al., 2013; Pither et al., 2021; Vorobeva et al., 2006). This suggests that SSA might play a role in modulating and priming immune responses, particularly in dampening the intensive activation of TLR-mediated proinflammatory cytokine signaling by pathogens. Furthermore, the IRF activation by SSA, crucial in the transcription of interferons and the induction of antiviral defenses, adds another dimension to the potential immunological effects of SSA exposure. This is especially interesting in light of recent epidemiological data suggesting lower rates of COVID-19 infections at the Italian coast (Cascetta et al., 2021), implying a possible link between SSA exposure and enhanced antiviral protection. Future investigation into the immunostimulatory benefits of SSA exposure with a focus on the two key areas mentioned above are recommended.

Previous studies used largely differing methodologies to acquire sufficient SSA for biological studies (Ferguson et al., 2019), hampering our ability to compare our results. Based on our own empirical experiences and suggestions by literature (de Sousa et al., 2020; Moretti, 2018), we used a Coriolis sampler operating at its maximum air flow rate (de Sousa et al., 2020; Moretti, 2018)and placed it directly adjacent to the sea to capture more and larger SSA droplets. The total bacterial counts in our Field samples (**Table S1**; ranging from 3.0×10^3 to 6.0×10^5 cells/m^3 air) align with those found at a coastal site in Japan (about 10^4 cells/m^3 air) (Fan et al., 2023), as well as those found in air over open sea regions such as the Mediterranean Sea (5×10^3 to 2×10^4 cells/m^3 air) (Mescioglu et al., 2019), the East Sea of Korea (about 10^5 cells/m^3 air) (Cho and Hwang, 2011), the Northwestern Pacific Ocean (1.0×10^4 to 2.5×10^5 cells/m^3 air) (Hu et al., 2017), the North Atlantic Ocean (2.8×10^3 to 1.9×10^4 cells/m^3 air) (Mayol et al., 2014), and the global tropical and subtropical ocean (10^3 to 10^4 cells/m^3 air) (Mayol et al., 2017). The only other study we found that investigated airborne endotoxin of

marine origin in coastal areas, reported endotoxin levels ranging from 0.0 to 3.6 EU/m^3 air over the coastal city of Haifa, Israel (Lang-Yona et al., 2014). The endotoxin levels in our Field SSA samples were high in comparison, ranging from 7 to 1,217 EU/m^3 air (**Fig. 2 (c), Table S1**). These levels are comparable to, and even surpass, those (0-16,720 EU/m^3 air) found in non-SSA dominated air samples from diverse background environments such as traffic zones, green spaces, agricultural areas, and industrial settings (e.g., poultry farms, lumber mills, wastewater treatment plants) (Madsen, 2006; Moretti et al., 2018). Besides the collection of larger and more SSA, which may contain more bacteria (Lighthart and Shaffer, 1997), a plausible explanation for this high value lies in the occurrence of spring phytoplankton blooms. A close coupling between bacterial numbers with phytoplankton biomass during the spring bloom has been reported in Ostend (Lancelot and Billen, 1984).

Besides the aforementioned sampling locality and sampling method, external factors such as meteorological parameters (e.g., wind speed, air temperature, relative humidity, and solar radiation) and background conditions (e.g., land-origin air, anthropogenic aerosols) also influence SSA composition and biomass (Su et al., 2022). To exclude as many external determinants as possible, we used the MART as a supplementary method to produce SSA with a high biomass and less background contaminations (Prather et al., 2013; Stokes et al., 2013). The MART samples consistently mirrored the weekly fluctuations of total bacterial counts and endotoxin concentrations observed in the Field samples (**Fig. 2 (a, b, c)**), underscoring the pivotal role of seawater biology. The total bacterial counts and endotoxin levels in the MART samples (**Table S1**; 7.3 ± 5.5 x10^5 cells/m^3 air and 1,310 ± 513 EU/m^3 air, respectively) were higher than those in the Field samples (2.0 ± 1.9 x10^5 cells/m^3 air and 389 ± 434 EU/m^3 air, respectively), indicating the effectiveness of MART as a controlled experimental setup for generating SSA with high biomass. If this tool was more widely adopted in other regions in the world, a better intercomparison of studies would be feasible.

By exposing human reporter cells to SSA and assessing the activation of immune receptors and transcription factors key for bacteria-host interactions, including TLR4, TLR2/6, NF-κB, and IRF, we gained valuable insights into the immunostimulatory activity of SSA. These findings contribute to the understanding of the potential health impacts of SSA exposure to humans. We used SSA samples with

a wide range of total bacterial counts and endotoxin concentrations, but accurately matching these amounts to the levels inhaled by humans in real-world environments is difficult. This is mainly due to the lack of data on actual SSA inhalation in natural settings, which exists regarding the quantity and content of SSA, but also for exposure levels. In our study, we used a single and short-term exposure of approximately 24 hours, which helps us understand immediate and intense immune responses, but does not consider chronic, lower-level exposure. Such long-term exposure is more relevant for coastal residents and should be considered in future approaches, together with investigations about the fate of SSA in the human respiratory system. Employing additional aerosol sampling methods, such as the six-stage Andersen cascade impactor (Andersen, 1958), can help to get more data about these realistic exposure scenarios. Designed to simulate human respiratory tract sampling based on the aerodynamic diameters of particles, this sampling device has been used to investigate concentrations of inhalable particle-bound marine biotoxins across different respiratory regions, such as the nasopharynx, tracheobronchial, and alveolar regions (Yu et al., 2022). Moreover, we recommend the application of more complex models for future approaches as well. In the present study, we used human reporter cell lines, which are engineered to measure activation of specific immune receptors and transcription factors. Though insightful, these reporter cells might not fully represent the complexity of human immune system, and its different cells, such as macrophages, dendritic cells, B cells, and T lymphocytes. One step further, expanding the model cells to include cultures of primary immune cells, especially those from the respiratory tract, and 3D cell cultures, which more closely mimic the actual architecture and microenvironment of human tissues, could provide more physiologically relevant data (Barrila et al., 2010; Crabbé et al., 2017). Finally, well-designed clinical trials and integrating a comprehensive range of biomarkers in future studies, from cellular signaling molecules and transcription factors to a diverse array of response indicators including cytokines, interferons, and cellular function markers, using advanced techniques like PCR array and transcriptomics, will be helpful for dissecting the complex cascade of effects triggered by SSA. Building up on the results demonstrated in this study, this inclusive approach will provide a holistic understanding of the multifaceted health effects of SSA and the underlying mechanisms involved.

5. Conclusions

This study advances our understanding of the immunological impacts of SSA exposure on several key receptors and transcription factors of the human immune system, paving the way for further research in this area of environmental health. Our findings reveal characteristics of specific microbial SSA components (i.e., total bacterial counts and endotoxin concentrations) and their importance for the activation of receptors TLR4 and TLR2/6, and transcription factors NF-κB and IRF that facilitate innate and adaptive immune responses. The correlations observed in this study underline the potential health implications of SSA exposure for populations in coastal areas. These insights suggest that the coastal health effects may extend beyond lifestyle factors by being related to continuous exposure to the diverse and complex marine substances present in SSA. To understand the potential immunological impacts highlighted by our findings, future research should broaden its scope to focus on the comprehensive biological and chemical compositions within SSA, including the consideration of seasonal changes and geographic variations. This includes evaluating a wide range of microbial entities and chemical constituents, and their combined or individual effects on a spectrum of biological responses beyond isolated aspects of immune system activation. Such a holistic approach will provide deeper insights into how various components of SSA contribute not only to immune activation but also to other physiological and potential pathophysiological processes. A comprehensive assessment of the risks and benefits associated with prolonged exposure to SSA is crucial for public health and environmental health research, especially for populations residing in coastal areas. Ultimately, a better understanding of the intricate interactions between SSA components and human health will inform effective environmental and health policies, enhancing our ability to explain, protect and improve the health of communities in these unique ecological settings.

Data Availability

The dataset produced and presented in this work, and the analysis code are openly available in the online repository Marine Data Archive, https://doi.org/10.14284/658.

Acknowledgement

Y.L. is funded by Flanders Marine Institute (VLIZ). M.D. is supported by Flanders Innovation & Entrepreneurship (VLAIO) through a Baekeland-mandate (HBC.2020.2287). I.S. is supported by Flanders Research Foundation through a personal postdoctoral grant (FWO 1277222N). We thank Emmy Pequeur (GhEnToxLab, Ghent University) for the measurement of sodium, and Thomas Pluym and Sam Decroo (CMET, Ghent University) for their help on the operation of flow cytometry.

References

Aller, J.Y., Kuznetsova, M.R., Jahns, C.J., Kemp, P.F., 2005. The sea surface microlayer as a source of viral and bacterial enrichment in marine aerosols. Journal of Aerosol Science 36, 801–812. https://doi.org/10.1016/j.jaerosci.2004.10.012

Andersen, A.A., 1958. NEW SAMPLER FOR THE COLLECTION, SIZING, AND ENUMERATION OF VIABLE AIRBORNE PARTICLES. Journal of Bacteriology 76, 471–484. https://doi.org/10.1128/jb.76.5.471-484.1958

Asselman, J., Van Acker, E., De Rijcke, M., Tilleman, L., Van Nieuwerburgh, F., Mees, J., De Schamphelaere, K.A.C., Janssen, C.R., 2019. Marine biogenics in sea spray aerosols interact with the mTOR signaling pathway. Scientific Reports 9. https://doi.org/10.1038/s41598-018-36866-3

Barrila, J., Radtke, A.L., Crabbé, A., Sarker, S.F., Herbst-Kralovetz, M.M., Ott, C.M., Nickerson, C.A., 2010. Organotypic 3D cell culture models: Using the rotating wall vessel to study host-pathogen interactions. Nature Reviews Microbiology 8, 791–801. https://doi.org/10.1038/nrmicro2423

Belgische, S., 2018. Actualisatie van de initiële beoordeling voor de Belgische mariene wateren. Kaderrichtlijn Mariene Strategie – Art 8 lid 1a & 1b: België 2018-2024. Available at https://odnature.naturalsciences.be/downloads/msfd/KRMS_Art8_2018.pdf.

Carillo, S., Pieretti, G., Parrilli, E., Tutino, M.L., Gemma, S., Molteni, M., Lanzetta, R., Parrilli, M., Corsaro, M.M., 2011. Structural investigation and biological activity of the lipooligosaccharide from the psychrophilic bacterium pseudoalteromonas haloplanktis TAB 23. Chemistry - A European Journal 17, 7053–7060. https://doi.org/10.1002/chem.201100579

Cascetta, E., Henke, I., Di Francesco, L., 2021. The Effects of Air Pollution, Sea Exposure and Altitude on COVID-19 Hospitalization Rates in Italy. International journal of environmental research and public health 18. https://doi.org/10.3390/ijerph18020452

Cheng, Y.S., Zhou, Y., Irvin, C.M., Pierce, R.H., Naar, J., Backer, L.C., Fleming, L.E., Kirkpatrick, B., Baden, D.G., 2005. Characterization of marine aerosol for assessment of human exposure to brevetoxins. Environmental Health Perspectives 113, 638–643. https://doi.org/10.1289/ehp.7496

Cho, B.C., Hwang, C.Y., 2011. Prokaryotic abundance and 16S rRNA gene sequences detected in marine aerosols on the East Sea (Korea). FEMS Microbiology Ecology 76, 327–341. https://doi.org/10.1111/j.1574-6941.2011.01053.x

Claes, I.J.J., Segers, M.E., Verhoeven, T.L.A., Dusselier, M., Sels, B.F., De Keersmaecker, S.C.J., Vanderleyden, J., Lebeer, S., 2012. Lipoteichoic acid is an important microbe-associated molecular pattern of Lactobacillus rhamnosus GG. Microbial Cell Factories 11, 2–9. https://doi.org/10.1186/1475-2859-11-161

Crabbé, A., Liu, Y., Matthijs, N., Rigole, P., De La Fuente-Nùñez, C., Davis, R., Ledesma, M.A., Sarker, S., Van Houdt, R., Hancock, R.E.W., Coenye, T., Nickerson, C.A., 2017. Antimicrobial efficacy against Pseudomonas aeruginosa biofilm formation in a three-dimensional lung epithelial model and the influence of fetal bovine serum. Scientific Reports 7, 1–13. https://doi.org/10.1038/srep43321

Darquenne, C., 2012. Aerosol deposition in health and disease. Journal of aerosol medicine and pulmonary drug delivery, 25(3), pp.140-147. https://doi.org/10.1089/jamp.2011.0916

De Leeuw, G., Neele, F.P., Hill, M., Smith, M.H., Vignati, E., 2000. Production of sea spray aerosol

in the surf zone. Journal of Geophysical Research Atmospheres 105, 29397–29409. https://doi.org/10.1029/2000JD900549

de Sousa, N.R., Shen, L., Silcott, D., Call, C.J., Rothfuchs, A.G., 2020. Operative and technical modifications to the coriolis® μ air sampler that improve sample recovery and biosafety during microbiological air sampling. Annals of Work Exposures and Health 64, 852–865. https://doi.org/10.1093/ANNWEH/WXAA053

Dempsey, S., Devine, M.T., Gillespie, T., Lyons, S., Nolan, A., 2018. Coastal blue space and depression in older adults. Health and Place 54, 110–117. https://doi.org/10.1016/j.healthplace.2018.09.002

Di Lorenzo, F., Palmigiano, A., Albitar-Nehme, S., Pallach, M., Kokoulin, M., Komandrova, N., Romanenko, L., Bernardini, M.L., Garozzo, D., Molinaro, A., Silipo, A., 2018. Lipid A Structure and Immunoinhibitory Effect of the Marine Bacterium Cobetia pacifica KMM 3879T. European Journal of Organic Chemistry 2018, 2707–2716. https://doi.org/10.1002/ejoc.201800279

Di Lorenzo, F., Palmigiano, A., Paciello, I., Pallach, M., Garozzo, D., Bernardini, M.L., La Cono, V., Yakimov, M.M., Molinaro, A., Silipo, A., 2017. The deep-sea polyextremophile Halobacteroides lacunaris TB21 rough-type LPS: Structure and inhibitory activity towards toxic LPS. Marine Drugs 15, 1–16. https://doi.org/10.3390/md15070201

Erridge, C., Bennett-Guerrero, E., Poxton, I.R., 2002. Structure and function of lipopolysaccharides. Microbes and Infection 4, 837–851. https://doi.org/10.1016/S1286-4579(02)01604-0

Facciponte, D.N., Bough, M.W., Seidler, D., Carroll, J.L., Ashare, A., Andrew, A.S., Tsongalis, G.J., Vaickus, L.J., Henegan, P.L., Butt, T.H., Stommel, E.W., 2018. Identifying aerosolized cyanobacteria in the human respiratory tract: A proposed mechanism for cyanotoxin-associated diseases. Science of the Total Environment 645, 1003–1013. https://doi.org/10.1016/j.scitotenv.2018.07.226

Fan, C., Xie, W., Hu, W., Matsusaki, H., Kojima, T., Zhang, D., 2023. Number size distribution of bacterial aerosols in terrestrial and marine airflows at a costal site of Japan. Science of the Total Environment 865, 161238. https://doi.org/10.1016/j.scitotenv.2022.161238

Ferguson, R.M.W., Garcia-Alcega, S., Coulon, F., Dumbrell, A.J., Whitby, C., Colbeck, I., 2019. Bioaerosol biomonitoring: Sampling optimization for molecular microbial ecology. Molecular Ecology Resources 19, 672–690. https://doi.org/10.1111/1755-0998.13002

Fox, J., Weisberg, S., 2011. An R Companion to Applied Regression-SAGE Publications. Sage publications.

Gustafsson, M.E.R., Franzén, L.G., 2000. Inland transport of marine aerosols in southern Sweden. Atmospheric Environment 34, 313–325. https://doi.org/10.1016/S1352-2310(99)00198-3

Hamed, I., Özogul, F., Özogul, Y., Regenstein, J.M., 2015. Marine Bioactive Compounds and Their Health Benefits: A Review. Comprehensive Reviews in Food Science and Food Safety 14, 446–465. https://doi.org/10.1111/1541-4337.12136

Hetland, R.B., Cassee, F.R., Låg, M., Refsnes, M., Dybing, E., Schwarze, P.E., 2005. Cytokine release from alveolar macrophages exposed to ambient particulate matter: Heterogeneity in relation to size, city an season. Particle and Fibre Toxicology 2. https://doi.org/10.1186/1743-8977-2-4

Hooyberg, A., Michels, N., Roose, H., Everaert, G., Mokas, I., Malina, R., Vanderhasselt, M., Henauw, S. De, 2023. The psychophysiological reactivity to beaches vs . to green and urban environments : insights from a virtual reality experiment. Journal of Environmental Psychology 91, 102103. https://doi.org/10.1016/j.jenvp.2023.102103

Hooyberg, A., Roose, H., Grellier, J., Elliott, L.R., Lonneville, B., White, M.P., Michels, N., De Henauw, S., Vandegehuchte, M., Everaert, G., 2020. General health and residential proximity to the coast in Belgium: Results from a cross-sectional health survey. Environmental Research 184, 109225. https://doi.org/10.1016/j.envres.2020.109225

Hu, W., Murata, K., Fukuyama, S., Kawai, Y., Oka, E., Uematsu, M., Zhang, D., 2017. Concentration and viability of airborne bacteria over the Kuroshio extension region in the northwestern pacific ocean: Data from three cruises. Journal of Geophysical Research: Atmospheres 122, 12,892-12,905. https://doi.org/10.1002/2017JD027287

Hubel, A., Spindler, R., Skubitz, A.P.N., 2014. Storage of human biospecimens: Selection of the optimal storage temperature. Biopreservation and Biobanking 12, 165–175. https://doi.org/10.1089/bio.2013.0084

Kang, S.S., Sim, J.R., Yun, C.H., Han, S.H., 2016. Lipoteichoic acids as a major virulence factor causing inflammatory responses via Toll-like receptor 2. Archives of Pharmacal Research 39, 1519–1529. https://doi.org/10.1007/s12272-016-0804-y

Kawai, T., Akira, S., 2010. The role of pattern-recognition receptors in innate immunity: Update on toll-like receptors. Nature Immunology 11, 373–384. https://doi.org/10.1038/ni.1863

Kokoulin, M.S., Kuzmich, A.S., Kalinovsky, A.I., Tomshich, S. V., Romanenko, L.A., Mikhailov, V. V., Komandrova, N.A., 2016. Structure and anticancer activity of sulfated O-polysaccharide from marine bacterium Cobetia litoralis KMM 3880T. Carbohydrate Polymers 154, 55–61. https://doi.org/10.1016/j.carbpol.2016.08.036

Kusiak, A., Brady, G., 2022. Bifurcation of signalling in human innate immune pathways to NF-kB and IRF family activation. Biochemical Pharmacology 205, 115246. https://doi.org/10.1016/j.bcp.2022.115246

Lancelot, C., Billen, G., 1984. Activity of heterotrophic bacteria and its coupling to primary production during the spring phytoplankton bloom in the southern bight of the North Sea. Limnology and Oceanography 29, 721–730. https://doi.org/10.4319/lo.1984.29.4.0721

Lang-Yona, N., Lehahn, Y., Herut, B., Burshtein, N., Rudich, Y., 2014. Marine aerosol as a possible source for endotoxins in coastal areas. Science of the Total Environment 499, 311–318. https://doi.org/10.1016/j.scitotenv.2014.08.054

Liebers, V., Raulf-Heimsoth, M., Brüning, T., 2008. Health effects due to endotoxin inhalation (review). Archives of Toxicology 82, 203–210. https://doi.org/10.1007/s00204-008-0290-1

Lighthart, B., Shaffer, B.T., 1997. Increased airborne bacterial survival as a function of particle content and size. Aerosol Science and Technology 27, 439–446. https://doi.org/10.1080/02786829708965483

Maaetoft-Udsen, K., Vynne, N., Heegaard, P.M., Gram, L., Frøkiær, H., 2013. Pseudoalteromonas strains are potent immunomodulators owing to low-stimulatory LPS. Innate Immunity 19, 160–173. https://doi.org/10.1177/1753425912455208

Madsen, A.M., 2006. Airborne Endotoxin in Different background environments and seasons. Annals of Agricultural and Environmental Medicine 13, 81–86.

Mayol, E., Arrieta, J.M.J.M., Jimenez, M.A., Martinez-Asensio, A., Garcias-Bonet, N., Dachs, J., Gonzalez-Gaya, B., Royer, S.-J.J., Benitez-Barrios, V.M., Fraile-Nuez, E., Duarte, C.M., Jiménez, M.A., Martínez-Asensio, A., Garcias-Bonet, N., Dachs, J., González-Gaya, B., Royer, S.-J.J., Benítez-Barrios, V.M., Fraile-Nuez, E., Duarte, C.M., 2017. Long-range transport of airborne microbes over the global tropical and subtropical ocean. Nature Communications 8, 1–8. https://doi.org/10.1038/s41467-017-00110-9

Mayol, E., Jiménez, M.A., Herndl, G.J., Duarte, C.M., Arrieta, J.M., 2014. Resolving the abundance and air- sea fluxes of airborne microorganisms in the North Atlantic Ocean. Frontiers in Microbiology 5, 1–10. https://doi.org/10.3389/fmicb.2014.00557

Mescioglu, E., Rahav, E., Belkin, N., Xian, P., Eizenga, J.M., Vichik, A., Herut, B., Paytan, A., 2019. Aerosol Microbiome over the Mediterranean Sea Diversity and Abundance. Atmosphere 10. https://doi.org/10.3390/atmos10080440

Moore, M.N., 2015. Do airborne biogenic chemicals interact with the PI3K/Akt/mTOR cell signalling pathway to benefit human health and wellbeing in rural and coastal environments? Environmental Research 140, 65–75. https://doi.org/10.1016/j.envres.2015.03.015

Moretti, S., 2018. Interplay of bacterial endotoxins and transition metals in the inflammatory capacity of airborne particulate matter. Thesis (Doctoral dissertation).

Moretti, S., Smets, W., Hofman, J., Mubiana, K.V., Oerlemans, E., Vandenheuvel, D., Samson, R., Blust, R., Lebeer, S., 2019. Human inflammatory response of endotoxin affected by particulate matter-bound transition metals. Environmental Pollution 244, 118–126. https://doi.org/10.1016/j.envpol.2018.09.148

Moretti, S., Smets, W., Oerlemans, E., Blust, R., Lebeer, S., 2018. The abundance of urban endotoxins as measured with an impinger-based sampling strategy. Aerobiologia 34, 487–496. https://doi.org/10.1007/s10453-018-9525-7

Nescerecka, A., Hammes, F., Juhna, T., 2016. A pipeline for developing and testing staining protocols for flow cytometry, demonstrated with SYBR Green I and propidium iodide viability staining. Journal of Microbiological Methods 131, 172–180. https://doi.org/10.1016/j.mimet.2016.10.022

Pither, M.D., Mantova, G., Scaglione, E., Pagliuca, C., Colicchio, R., Vitiello, M., Chernikov, O. V., Hua, K.F., Kokoulin, M.S., Silipo, A., Salvatore, P., Molinaro, A., Di Lorenzo, F., 2021. The unusual lipid a structure and immunoinhibitory activity of LPS from marine bacteria echinicola pacifica KMM 6172T and echinicola Vietnamensis KMM 6221T. Microorganisms 9, 1–18. https://doi.org/10.3390/microorganisms9122552

Prather, K.A., Bertram, T.H., Grassian, V.H., Deane, G.B., Stokes, M.D., DeMott, P.J., Aluwihare, L.I., Palenik, B.P., Azam, F., Seinfeld, J.H., Moffet, R.C., Molina, M.J., Cappa, C.D., Geiger, F.M., Roberts, G.C., Russell, L.M., Ault, A.P., Baltrusaitis, J., Collins, D.B., Corrigan, C.E., Cuadra-Rodriguez, L.A., Ebben, C.J., Forestieri, S.D., Guasco, T.L., Hersey, S.P., Kim, M.J., Lambert, W.F., Modini, R.L., Mui, W., Pedler, B.E., Ruppel, M.J., Ryder, O.S., Schoepp, N.G., Sullivan, R.C., Zhao, D., 2013. Bringing the ocean into the laboratory to probe the chemical complexity of sea spray aerosol. Proceedings of the National Academy of Sciences of the United States of America 110, 7550–7555. https://doi.org/10.1073/pnas.1300262110

Rastelli, E., Corinaldesi, C., Dell'anno, A., Lo Martire, M., Greco, S., Cristina Facchini, M., Rinaldi,

M., O'Dowd, C., Ceburnis, D., Danovaro, R., 2017. Transfer of labile organic matter and microbes from the ocean surface to the marine aerosol: An experimental approach. Scientific Reports 7. https://doi.org/10.1038/s41598-017-10563-z

Spacova, I., De Boeck, I., Cauwenberghs, E., Delanghe, L., Bron, P.A., Henkens, T., Simons, A., Gamgami, I., Persoons, L., Claes, I., van den Broek, M.F.L., Schols, D., Delputte, P., Coenen, S., Verhoeven, V., Lebeer, S., 2023. Development of a live biotherapeutic throat spray with lactobacilli targeting respiratory viral infections. Microbial Biotechnology 16, 99–115. https://doi.org/10.1111/1751-7915.14189

Steerenberg, P.A., Withagen, C.E.T., Van Dalen, W.J., Dormans, J.A.M.A., Cassee, F.R., Heisterkamp, S.H., Van Loveren, H., 2004. Adjuvant activity of ambient particulate matter of different sites, sizes, and seasons in a respiratory allergy mouse model. Toxicology and Applied Pharmacology 200, 186–200. https://doi.org/10.1016/j.taap.2004.04.011

Stein, A.F., Draxler, R.R., Rolph, G.D., Stunder, B.J.B., Cohen, M.D., Ngan, F., 2015. NOAA's HYSPLIT atmospheric transport and dispersion modeling system. Bulletin of the American Meteorological Society 96, 2059–2077. https://doi.org/10.1175/BAMS-D-14-00110.1

Stokes, M.D., Deane, G.B., Prather, K., Bertram, T.H., Ruppel, M.J., Ryder, O.S., Brady, J.M., Zhao, D., 2013. A Marine Aerosol Reference Tank system as a breaking wave analogue for the production of foam and sea-spray aerosols. Atmospheric Measurement Techniques 6, 1085–1094. https://doi.org/10.5194/amt-6-1085-2013

Su, B., Wang, T., Zhang, G., Liang, Y., Lv, C., Hu, Y., Li, L., Zhou, Z., Wang, X., Bi, X., 2022. A review of atmospheric aging of sea spray aerosols: Potential factors affecting chloride depletion. Atmospheric Environment 290, 119365. https://doi.org/10.1016/j.atmosenv.2022.119365

Suleria, H.A.R., Gobe, G., Masci, P., Osborne, S.A., 2016. Marine bioactive compounds and health promoting perspectives; innovation pathways for drug discovery. Trends in Food Science and Technology 50, 44–55. https://doi.org/10.1016/j.tifs.2016.01.019

Taniguchi, T., Ogasawara, K., Takaoka, A., Tanaka, N., 2001. IRF family of transcription factors as regulators of host defense. Annual review of immunology 19, 623–655. https://doi.org/10.1146/annurev.immunol.19.1.623

Van Acker, E., De Rijcke, M., Liu, Z., Asselman, J., De Schamphelaere, K.A.C., Vanhaecke, L., Janssen, C.R., 2021a. Sea Spray Aerosols Contain the Major Component of Human Lung Surfactant. Environmental Science and Technology 55, 15989–16000. https://doi.org/10.1021/acs.est.1c04075

Van Acker, E., Huysman, S., De Rijcke, M., Asselman, J., De Schamphelaere, K.A.C., Vanhaecke, L., Janssen, C.R., 2021b. Phycotoxin-Enriched Sea Spray Aerosols: Methods, Mechanisms, and Human Exposure. Environmental Science and Technology 55, 6184–6196. https://doi.org/10.1021/acs.est.1c00995

Van Nevel, S., Koetzsch, S., Weilenmann, H.U., Boon, N., Hammes, F., 2013. Routine bacterial analysis with automated flow cytometry. Journal of Microbiological Methods 94, 73–76. https://doi.org/10.1016/j.mimet.2013.05.007

Vorobeva, E. V., Krasikova, I.N., Solov'eva, T.F., 2006. Influence of lipopolysaccharides and lipids A from some marine bacteria on spontaneous and Escherichia coli LPS-induced TNF-α release from peripheral human blood cells. Biochemistry (Moscow) 71, 759–766. https://doi.org/10.1134/S000629790607008X

Wheeler, B.W., White, M., Stahl-Timmins, W., Depledge, M.H., 2012. Does living by the coast improve health and wellbeing. Health and Place 18, 1198–1201. https://doi.org/10.1016/j.healthplace.2012.06.015

White, M.P., Pahl, S., Wheeler, B.W., Fleming, L.E.F., Depledge, M.H., 2016. The "Blue Gym": What can blue space do for you and what can you do for blue space? Journal of the Marine Biological Association of the United Kingdom 96, 5–12. https://doi.org/10.1017/S0025315415002209

Yu, S., Zhou, X., Hu, P., Chen, H., Shen, F., Yu, C., Meng, H., Zhang, Y., Wu, Y., 2022. Inhalable Particle-bound Marine Biotoxins in a Coastal Atmosphere: Concentration Levels, Influencing Factors and Health Risks. Journal of Hazardous Materials 434, 128925. https://doi.org/10.1016/j.jhazmat.2022.128925

Zeileis, A., Hothorn, T., 2002. Diagnostic Checking in Regression Relationships 2.

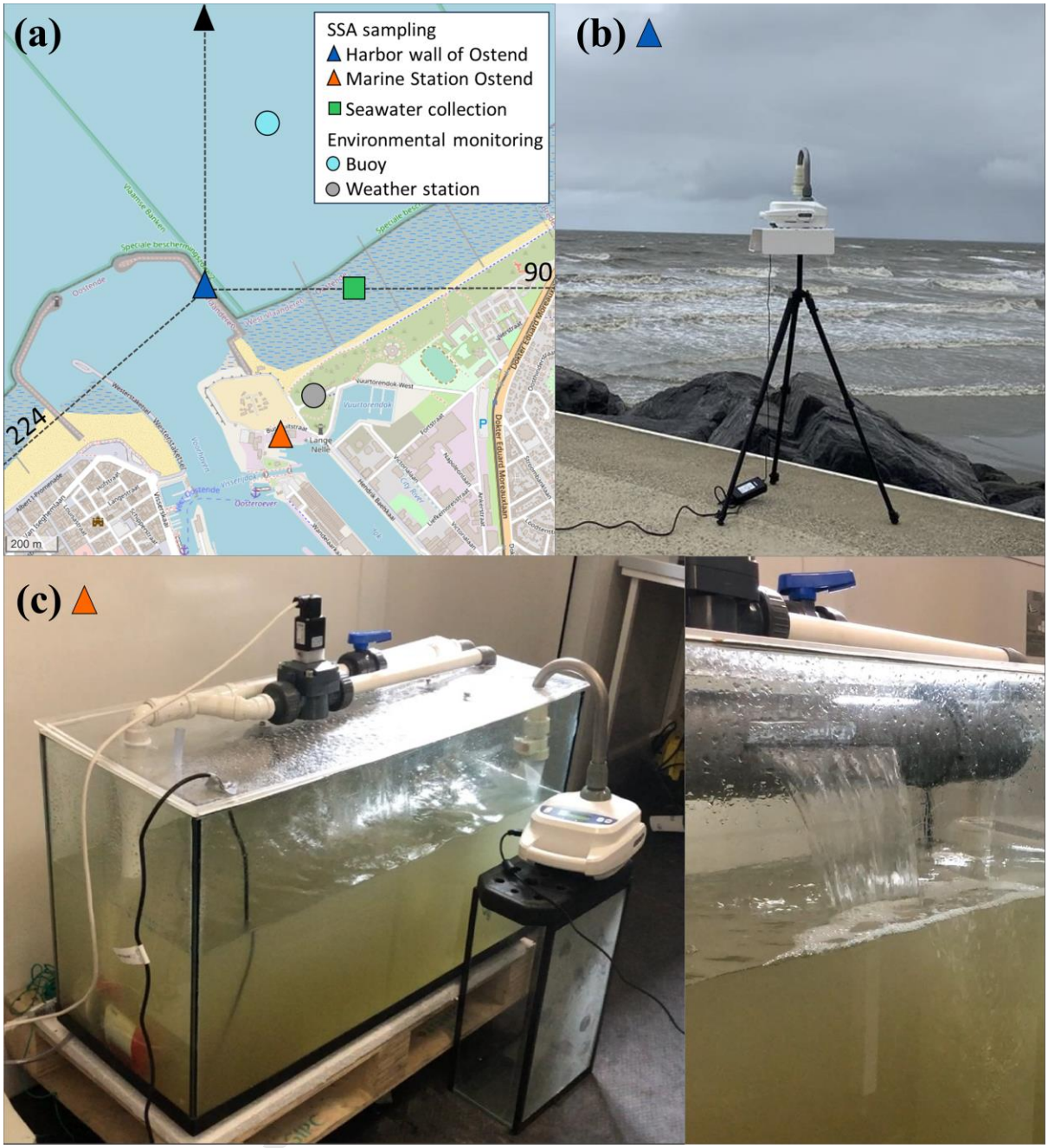

Fig. 1. (a) Map showing the locations of field sea spray aerosols (SSA) sampling on the harbor wall of Ostend (HO), the Marine Station Ostend (MSO), the seawater collection site for laboratory SSA generation, and the local environmental monitoring stations (Buoy and Weather station). Sea wind directions for HO are between ≥224° and ≤90°. (b) Field SSA sampling on the HO using a Coriolis sampler. (c) SSA generation at the MSO using a marine aerosol reference tank (MART).

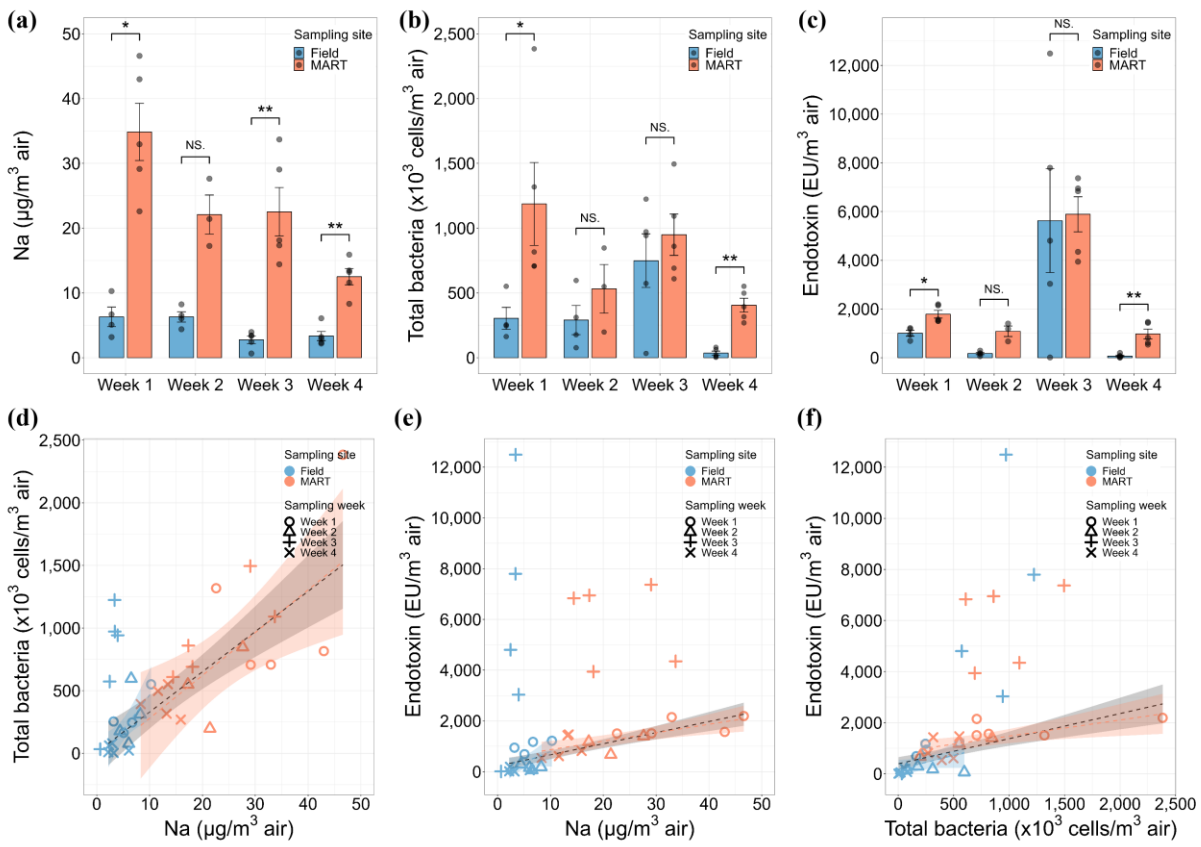

Fig. 2. Bar plots displaying (a) sodium (Na) content, (b) total bacterial count, and (c) endotoxin concentration in sea spray aerosols (SSA) samples collected from different sites (Field and MART) across different weeks (Weeks 1, 2, 3, and 4). Differences among groups were tested using the Kruskal-Wallis test followed by the Wilcoxon rank sum test. NS., not significant; *, $p < 0.05$; **, $p < 0.01$. Linear regression correlations with 95% confidence intervals between (d) Na content and total bacterial count, (e) Na content and endotoxin concentration, and (f) total bacterial count and endotoxin concentration were added as dashed lines. Regression lines for Field samples, MART samples, and combined samples were colored blue, orange, and black, respectively. Week 3 data were omitted from these regression analyses due to suspected terrestrial origins.

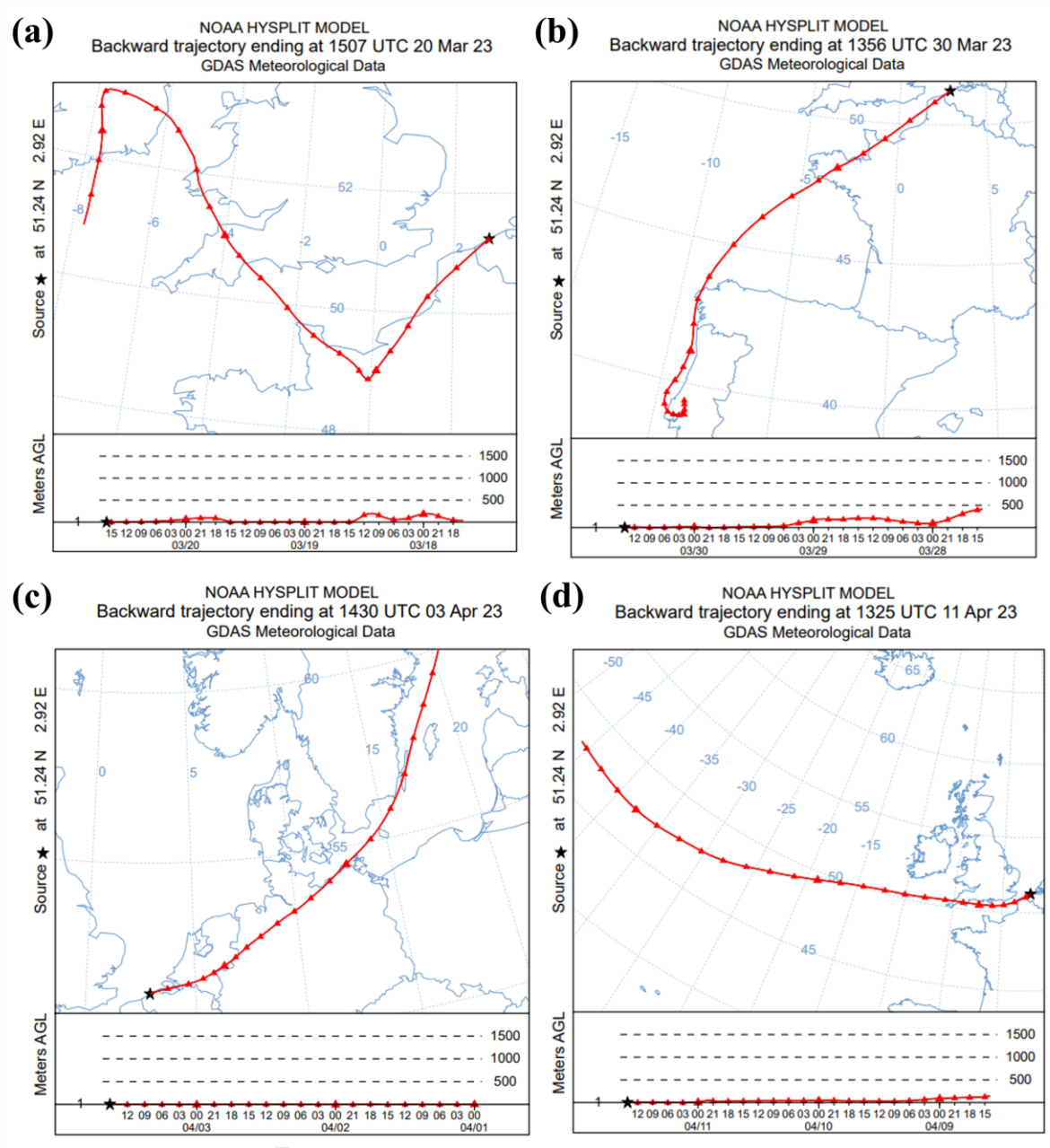

Fig. 3. 72-hour back trajectories of air masses arriving at the sampling height on the harbor wall of Ostend (HO) for each field sampling period in (a) Week 1, (b) Week 2, (c) Week 3, and (d) Week 4. These trajectories were calculated using the Hybrid Single-Particle Lagrangian Integrated Trajectory model (HYSPLIT) model with Global Data Assimilation System (GDAS) meteorological data.

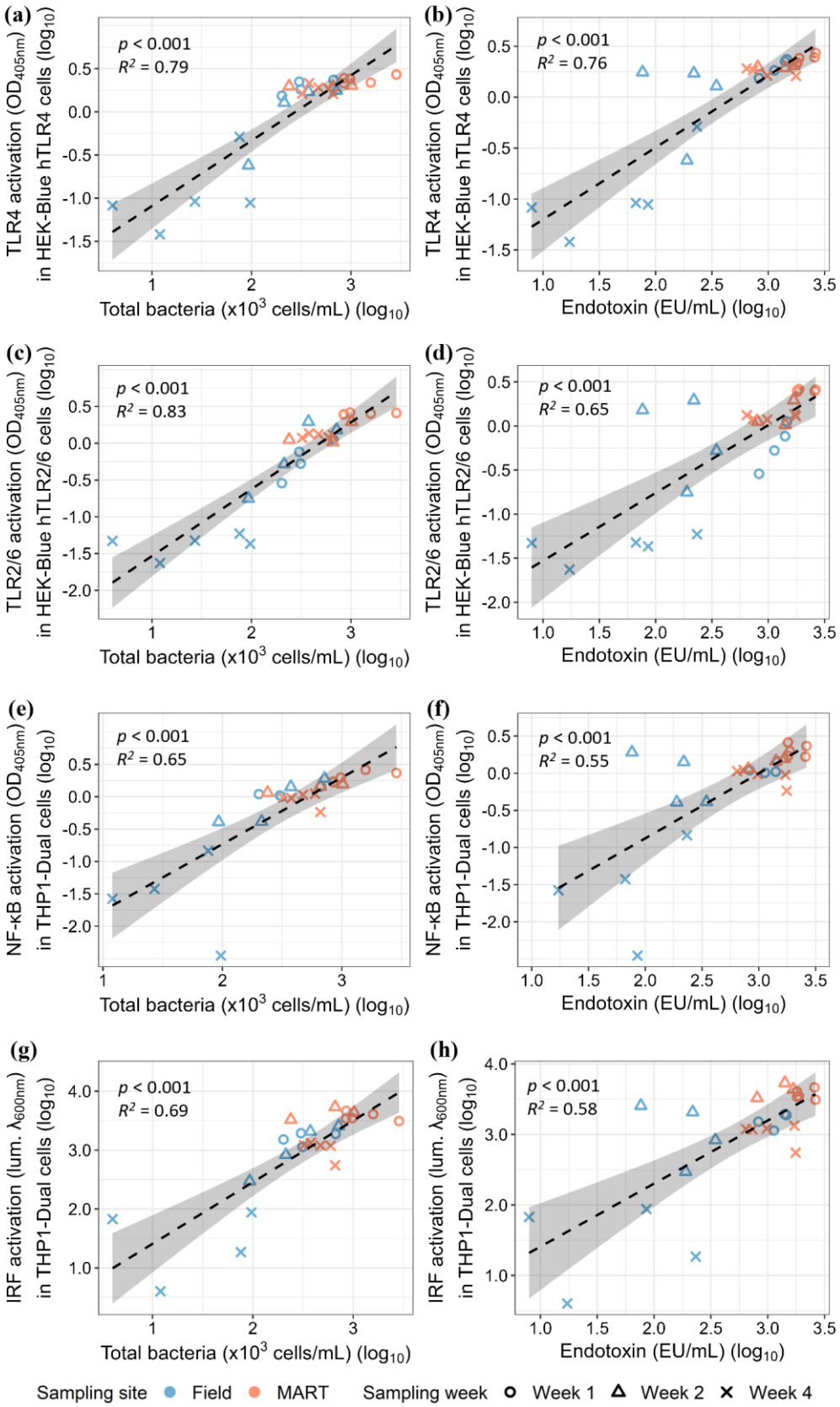

Fig. 4. Linear regressions with 95% confidence intervals between $\log_{10}$-transformed values of total bacterial count and endotoxin concentration with the activations of TLR4 in HEK-Blue hTLR4 cells, TLR2/6 in HEK-Blue hTLR2/6 cells, and NF-κB and IRF in THP1-Dual cells, induced by SSA.

Graphical abstract

0

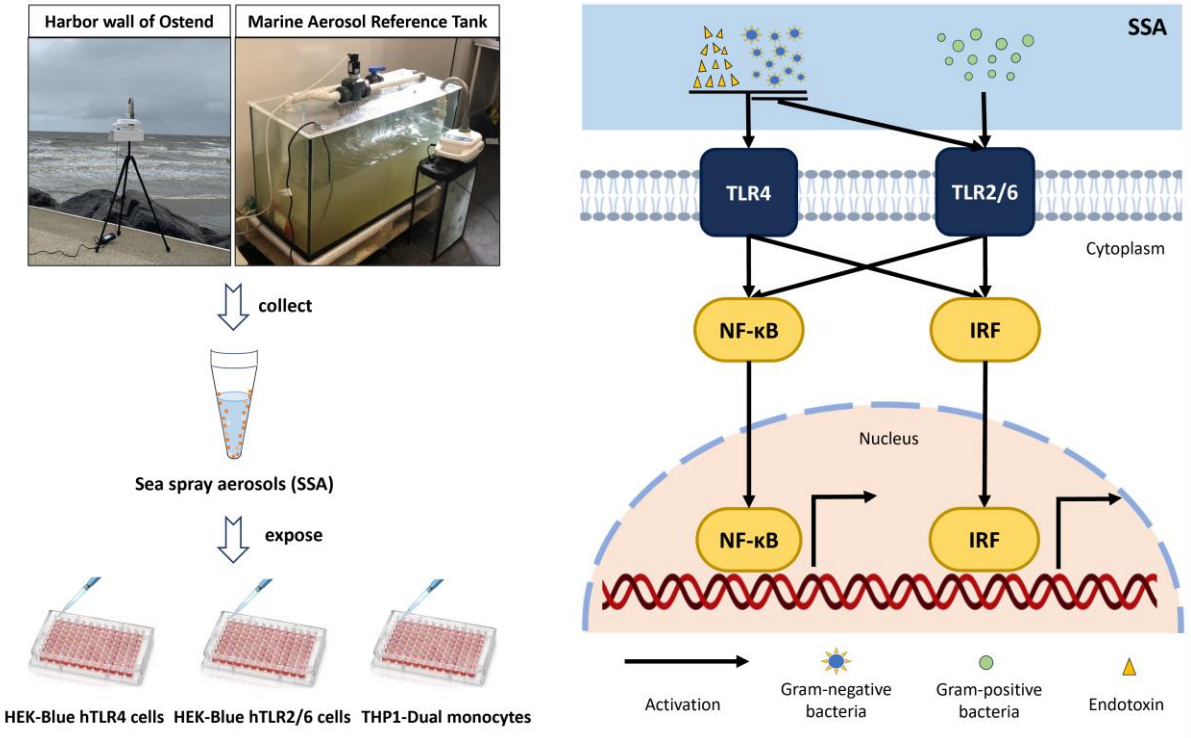

Highlights

- We studied the immunostimulatory activity of field and generated sea spray aerosols.
- Sea spray aerosols activated TLR4, TLR2/6, NF-κB and IRF in human cells.
- Immune responses demonstrated dose-dependence on bacterial components.
- Our findings reveal potential health implications of sea spray aerosols exposure.